

# How Understanding Forecast Uncertainty Resolves the Explainability Problem in Machine Learning Models

Joseph L. Breeden

19 August 2025

## Abstract

For applications of machine learning in critical decisions, explainability is a primary concern, and often a regulatory requirement. Local linear methods for generating explanations, such as LIME and SHAP, have been criticized for being unstable near decision boundaries. In this paper, we explain that such concerns reflect a misunderstanding of the problem. The forecast uncertainty is high at decision boundaries, so consequently, the explanatory instability is high. The correct approach is to change the sequence of events and questions being asked. Nonlinear models can be highly predictive in some regions while having little or no predictability in others. Therefore, the first question is whether a usable forecast exists. When there is a forecast with low enough uncertainty to be useful, an explanation can be sought via a local linear approximation. In such cases, the explanatory instability is correspondingly low. When no usable forecast exists, the decision must fall to a simpler overall model such as traditional logistic regression. Additionally, these results show that some methods that purport to be explainable everywhere, such as ReLU networks or any piecewise linear model, have only an illusory explainability, because the forecast uncertainty at the segment boundaries is too high to be useful. Explaining an unusable forecast is pointless.

## 1 Introduction

The explainability problem in machine learning models has become increasingly important as complex algorithms are deployed in critical decision-making applications. Particularly in loan underwriting situations, regulatory concerns about explainability have been a direct drag on adoption. Even though the academic literature on credit risk modeling for loan underwriting is quite extensive [6], live deployments are comparatively sparse. Traditional approaches to model interpretability often rely on creating local linear models based on nearby data points to understand dominant attributes in predictions [37, 27, 35]. However, this approach becomes unstable near high-curvature regions and discontinuities in the objective function. This has led to a general criticism of machine learning models being inherently unexplainable [25], or to the creation of linearized alternatives [9, 29] with apparently greater explainability.

In the quest for explainability to meet regulatory requirements, machine learning deployments rarely consider forecast uncertainty. Unlike the linear models with which business

teams are accustomed, nonlinear models can have dramatically varying forecast uncertainty. In fact, the great power of machine learning models is in finding pockets of predictability within the state space, which implies that there are regions of lower or no predictability.

When taken together, machine learning models do not have an explainability problem. This paper shows that there is a general correspondence between explanatory stability and forecast uncertainty. When the forecast is poor, the explanatory power is low. This should not be surprising, but it makes clear that the use of machine learning models has been flawed, not the models themselves. When a forecast is generated, the first test should be of the forecast uncertainty, not the explanation. If the forecast uncertainty is unusably high, then no explanation is needed. The explanatory problem in machine learning is actually a user problem. When there is no forecast, there is no point in asking what drives this forecast.

Both high forecast uncertainty and high explanatory instability are caused in part by high curvature regions of the objective function, which will be demonstrated below. Looking at the forecast uncertainty in a local-linear approximation, such as in LIME [32], correctly identifies problematic regions. This does not reflect a problem with LIME, but rather a region where no forecast is available.

Just as nonlinear models are not as unexplainable as was thought, piecewise-linear models are not as explainable as is commonly assumed. Among the most popular explainable machine learning models in credit risk are few-layer neural networks with ReLU (Rectified Linear Unit) activation functions [4]. The purported explainability comes from the design feature that a linear model is directly estimated for each segment of the input feature space. Any forecast point has an unambiguous linear model with which to obtain the explanation. However, this explainability is illusory. If one takes a point near a segment boundary and considers natural input perturbations, the boundary discontinuities represent the same explanatory instability and underlying forecast uncertainties present in more nonlinear models.

This paper describes the theoretical basis of these observations and presents multiple examples of the correlation between explanatory instability and forecast uncertainty. Empirically, this suggests a universal functional relationship between the two. The paper concludes with a discussion of how machine learning models should be used in practice with a better understanding of their forecast limitations and where fallback methods are required.

## 2 Background

In consumer lending, model explainability is not primarily an academic preference but an operational requirement. Credit decisions must be defensible to regulators, auditable under model risk management, and communicable to consumers through adverse-action reasoning. In practice, however, many debates about explainability implicitly assume that the model output is locally reliable everywhere in the feature space. This assumption is often false for modern nonlinear machine learning models, whose predictive performance can vary sharply across applicants and regions of the input space.

This paper adopts the view that explainability is conditional on forecast usability. When predictive uncertainty is high, as it often is near decision thresholds, in sparse-data regions, or at boundaries induced by nonlinear structure, small, plausible perturbations to an applicant profile can produce materially different predictions, and therefore materially different

local explanations. In these settings, explanation instability is not a separate defect to be patched. It is a symptom of limited local predictability. A lending workflow that treats explanations as primary, while ignoring uncertainty, risks producing stable-sounding narratives for forecasts that are not decisionable. Accordingly, we review (i) established uncertainty quantification methods and (ii) standard robustness metrics for explanations, emphasizing how they interact in lending-style thresholded decisions.

A large body of work in explainable AI (XAI) focuses on producing local feature attributions (e.g., LIME and SHAP) as a proxy for “reasons” behind an individual prediction [32, 26]. In lending, however, explanations often serve at least two distinct downstream goals: (i) to satisfy governance and compliance expectations for transparency, auditability, and adverse-action communication, and (ii) to support actionable guidance to applicants (“what would need to change for approval?”). These goals do not always align, and each interacts differently with predictive uncertainty.

## 2.1 Counterfactual Explanations and Algorithmic Recourse

Counterfactual explanations aim to identify a minimal change to an input  $x$  that would flip a model decision, thereby producing an “actionable” narrative suitable for consumer-facing contexts [40]. Related work on algorithmic recourse formalizes and operationalizes this idea, emphasizing feasibility constraints and the distinction between mutable and immutable features [38]. In practice, both counterfactuals and recourse depend critically on the local geometry of the decision boundary. When forecast uncertainty is high near that boundary, recourse recommendations can become unstable or inconsistent.

## 2.2 Limits of Post-hoc Explanations in High-stakes Decisions

A complementary literature argues that, for high-stakes settings, reliance on post-hoc explanations of black-box models can be fragile or misleading, and that interpretable model classes may be preferable when performance permits [34, 25]. Empirical work has also shown that some attribution-style explanations can fail basic sanity checks (e.g., producing similar saliency maps for randomized networks), reinforcing the importance of verification and robustness testing [1, 2].

## 2.3 Calibration and Decision-grade Probabilities

Even when a model is accurate in ranking risk, the numerical outputs may be poorly calibrated, which matters for thresholded decisions, pricing, and downstream policy rules. Modern calibration techniques (e.g., temperature scaling) and diagnostic tools such as reliability diagrams emphasize that predictive probabilities should be evaluated and corrected, rather than assumed [20]. In the present work, calibration is distinct from the local uncertainty measures we study, but it is a necessary precondition for interpreting probabilities as decisionable quantities.

## 2.4 Model Risk Management Context

Finally, lending models operate within formal model risk management and supervisory regimes that require documented limitations, monitoring, and controls, especially when models influence credit access and pricing. While the regulatory details vary by jurisdiction, supervisory guidance typically emphasizes that model use should be commensurate with model limitations and uncertainty [15, 30]. This governance framing motivates the central thesis of this paper. Explanations should be sought only after establishing that a usable forecast exists.

# 3 Forecast Uncertainty Estimation Methods

Quantifying the forecast uncertainty of logistic regression or machine learning models is crucial for their safe deployment, especially in risk-sensitive fields such as lending or healthcare. Uncertainty estimates reveal where a model’s predictions may be unreliable, guiding both end-users and model developers towards more trustworthy, actionable results.

Uncertainty is generally assumed to be caused by randomly distributed noise, but may also be unmodelable structure [18, 31]. Accurate model selection and deployment involve capturing both types whenever possible.

Bayesian neural networks (BNNs) extend classical models by placing probabilistic priors on weights, producing a distribution over predictions that reflects epistemic uncertainty [5, 28, 19]. Exact Bayesian inference is intractable in practice, but scalable approximations, such as variational inference and Markov Chain Monte Carlo, enable practical usage for moderate-sized networks.

Monte Carlo dropout for neural networks interprets dropout applied at inference as approximate Bayesian model averaging [17]. By stochastically masking neurons during prediction, multiple forward passes yield a distribution over outputs whose mean and variance quantify predictive uncertainty. MC dropout is popular for its simplicity and effectiveness with minimal architectural adjustment.

Deep ensembles comprise collections of independently trained models; their predictive spread estimates epistemic uncertainty [24]. While computationally demanding, ensembles have empirically outperformed many Bayesian methods for uncertainty quantification and are preferred when reliability is essential.

Quantile regression directly models specified quantiles of target variables, so empirical prediction intervals can be extracted without explicit distributional assumptions [23]. Quantile regression is robust to heteroscedasticity, requires only minor model changes, and is valuable in both regression and probabilistic classification settings.

Conformal prediction provides distribution-free, statistically valid prediction intervals by calibrating model residuals on validation sets [39]. Given a coverage level, conformal intervals are guaranteed, under the assumption of exchangeability, to contain the true response with high probability. This method is model-agnostic and widely used in applied domains.

Local approximation methods (e.g., LIME) quantify forecast uncertainty by the error between the full model and a local surrogate, often using a weighted RMSE [33]. High local error flags regions of high epistemic uncertainty and poor local predictability. Both

conformal prediction and local linear uncertainty are tested here.

### 3.1 Measures of Explanatory Stability

The stability and robustness of machine learning explanations is a core concern in high-risk decisioning applications. This section briefly reviews standard and emerging quantitative measures of explanatory stability.

A widely recognized approach for quantifying explanatory robustness is the use of local Lipschitz estimates for the explanation map. For an explanation mapping  $\mathcal{E}$  evaluated at input  $x$ , a local Lipschitz constant  $L$  satisfies

$$\|\mathcal{E}(x_1) - \mathcal{E}(x_2)\| \leq L\|x_1 - x_2\| \quad (1)$$

for all  $x_1, x_2$  in a small neighborhood [2, 41, 10]. A low Lipschitz value indicates that similar inputs have similar explanations, capturing a formal notion of stability or robustness. Contemporary toolkits and theoretical work have extended this to handle rich input modalities and multivariate maps.

Evaluation of fidelity is another benchmark for explanation quality and robustness. Fidelity tests whether attributions co-vary with true model output under perturbations, while infidelity measures the expected discrepancy between attributed feature effects and observed output changes under designed perturbations [43, 42]. Sensitivity metrics assess explanation volatility under small input noise. Lower infidelity and sensitivity values are desirable, and both are increasingly adopted in large-scale benchmarks [36].

Repeated perturbations or retrainings commonly yield different feature-importance orderings. Stability in these rankings is often quantified via top- $K$  feature-set overlap, using measures such as the Jaccard index or Kendall’s  $\tau$  [22, 13, 11]. High overlap indicates robust, repeatable explanations, and these measures are widely used in practical interpretability toolkits. The concept parallels but is distinct from covariance-based instability: rank agreement summarizes the stability of which features are emphasized, rather than the magnitude or direction of the attribution.

The Rashomon set refers to the existence of many distinct models with similar predictive accuracy but potentially divergent explanations [8, 14, 12, 44]. Structural instability across this set means that, even if a model’s predictions are stable, the reasoning underlying them, i.e., the attribution or feature-importance routine, may be highly variable across near-optimal models.

For the current analysis, Lipschitz estimates and the Jaccard Top-k index will both be studied. In addition, new metrics are developed based upon the curvature of the feature space according to the Hessian matrix.

## 4 Quantifying Forecast Uncertainty

Many measures of forecast uncertainty and explanatory instability already exist. In principle, any combination of these could be used in order to study the relationship between uncertainty and instability. However, choosing complimentary definitions will allow both numerical and

theoretical comparisons. This approach combines geometric (curvature-based) and statistical (variance/covariance) perspectives.

The most important first step is to establish precise definitions of forecast uncertainty and explanatory instability. Since LIME is a widely used approach for credit risk model explainability, it makes sense to develop these metrics relative to a local linear approximation [32].

Let  $f : \mathbb{R}^N \rightarrow \mathbb{R}$  be a black-box model and  $\mathbf{x} \in \mathbb{R}^N$  be an input instance. In the LIME framework, we fit a linear surrogate model  $g(\mathbf{z}) = \boldsymbol{\beta}^\top \mathbf{z}$  by minimizing a weighted least squares objective.

$$\boldsymbol{\beta} = \arg \min_{\boldsymbol{\beta}} \sum_{i=1}^k w_i (f(\mathbf{z}^{(i)}) - \boldsymbol{\beta}^\top \mathbf{z}^{(i)})^2, \quad (2)$$

where  $\mathbf{z}^{(i)}$  are samples from a local perturbation distribution  $\pi(\cdot | \mathbf{x})$ , and  $w_i = \exp\left(-\frac{\|\mathbf{z}^{(i)} - \mathbf{x}\|^2}{\sigma^2}\right)$  are Gaussian weights centered at  $\mathbf{x}$ .

Two main approaches are tested for effectiveness in measuring forecast uncertainty: local linear uncertainty and conformal uncertainty.

## 4.1 Local Linear Uncertainty

In this analysis, following the LIME nomenclature, the local *Forecast Uncertainty* at  $\mathbf{x}$  is taken as the weighted root mean squared error (RMSE) of the surrogate model.

$$\text{Uncertainty}(\mathbf{x}) = \sqrt{\frac{\sum_{i=1}^k w_i (f(\mathbf{z}^{(i)}) - \boldsymbol{\beta}^\top \mathbf{z}^{(i)})^2}{\sum_{i=1}^k w_i}}. \quad (3)$$

This value estimates how well a local linear approximation explains the behavior of the original model in the vicinity of  $\mathbf{x}$ . Higher uncertainty suggests nonlinearities or instability in the model response surface near  $\mathbf{x}$ . This uncertainty measure is essentially a confidence interval normalized to units of standard deviation.

## 4.2 Conformal Uncertainty Estimation

Conformal prediction offers a model-agnostic framework for characterizing pointwise prediction uncertainty. In local explainability settings, this methodology is adapted to empirically estimate uncertainty surrounding an input  $\mathbf{x}_0$  by analyzing the model's behavior under a distribution of local perturbations. Specifically, conformal uncertainty at  $\mathbf{x}_0$  is assessed by generating a set of perturbed instances  $\{\mathbf{x}_0^{(j)}\}_{j=1}^M$ , where each perturbation is defined as  $\mathbf{x}_0^{(j)} = \mathbf{x}_0 + \boldsymbol{\epsilon}_j$  with  $\boldsymbol{\epsilon}_j$  independently drawn from a multivariate normal distribution centered at zero and with covariance  $\sigma_{\text{pert}}^2 \mathbf{I}$ . The predictions of the underlying model,  $f(\mathbf{x}_0^{(j)})$ , evaluated over these perturbed samples, are then used to summarize local output variability.

In practical simulation and analysis (such as in R implementations), several empirical statistics are computed to capture the distributional characteristics of these local predictions.

The standard deviation (SD) of the predictive values provides a direct quantification of local dispersion, formally computed as

$$\text{SD}(\mathbf{x}_0) = \sqrt{\frac{1}{M-1} \sum_{j=1}^M \left( f(\mathbf{x}_0^{(j)}) - \bar{f} \right)^2} \quad (4)$$

where  $\bar{f}$  denotes the mean of  $f(\mathbf{x}_0^{(j)})$  across all  $M$  perturbations. The interquartile range (IQR) is also often reported, calculated as the difference between the empirical 75th and 25th percentiles of the prediction set, thereby providing a robust measure of central spread less sensitive to outliers.

In addition to these, interval-based summary statistics are frequently used to provide operational uncertainty bounds. The empirical range,

$$\text{Range}(\mathbf{x}_0) = \max_j f(\mathbf{x}_0^{(j)}) - \min_j f(\mathbf{x}_0^{(j)}), \quad (5)$$

offers an informal but interpretable indicator of maximal potential prediction variability in the local neighborhood. For formal coverage, one may construct symmetric or quantile-based predictive intervals. For example, a 90% conformal interval is defined by the interval between the 5th and 95th percentiles,

$$[Q_{0.05}, Q_{0.95}], \quad (6)$$

where  $Q_p$  indicates the  $p$ th percentile of the local prediction distribution.

These empirical measures of conformal uncertainty, calculated nonparametrically from sampled perturbations, provide model-agnostic diagnostics of local output volatility. High values indicate regions of the input space where even minor changes to input variables can yield pronounced differences in model predictions, thus flagging areas of heightened prediction risk or model instability. By contrast, low values characterize local neighborhoods where the model's output response is relatively stable. Notably, this approach to uncertainty quantification is agnostic to the form, smoothness, or complexity of the underlying model, and can be consistently applied for comparative model analysis and for identifying input regions requiring caution in automated decision-making systems.

## 5 Quantifying Explanatory Instability

“Explainability” is not well defined in common usage. Some model users will be referring to whether an explanation can be found. This can be a problem when the forecast is the result of the combination of many mildly predictive features with nothing sufficiently dominant to be confidently reported as a cause. Others will be concerned about the stability of an explanation, usually meaning that small perturbations of the inputs can result in changes in the identified cause. The current research was motivated by the hypothesis that these situations are most likely to arise when the underlying forecast has high uncertainty. For the present investigation, the term “explanatory instability” is adopted as a more precise definition for what is meant by failing to have an explainable forecast.

## 5.1 Lipschitz-Based Local Sensitivity Metric

The Lipschitz metric is designed to quantify the local sensitivity of a predictive model near an input instance with respect to small perturbations of the feature vector. In the context of explainability, the local Lipschitz constant provides a natural summary of how much the model output can change in response to minor variations in the input, reflecting the local steepness or slope of the response surface.

Mathematically, for a differentiable function  $f : \mathbb{R}^N \rightarrow \mathbb{R}$ , the *pointwise Lipschitz constant* at  $\mathbf{x}_0$  is given by the norm of the gradient:

$$L_{\text{local}}(\mathbf{x}_0) = \|\nabla f(\mathbf{x}_0)\|, \quad (7)$$

where  $\|\cdot\|$  denotes the Euclidean norm. In practice, for black-box models and for feature spaces where analytic gradients are unavailable, this quantity can be empirically estimated using a set of perturbed samples  $\{\mathbf{x}_0^{(j)}\}_{j=1}^M$  around the input  $\mathbf{x}_0$ .

A common computational scheme employs a local linear surrogate model fit over the perturbed neighborhood, as in LIME. The surrogate's coefficient vector,  $\hat{\beta}(\mathbf{x}_0)$ , provides an estimated local gradient. The Lipschitz metric is then estimated as

$$\hat{L}(\mathbf{x}_0) = \|\hat{\beta}(\mathbf{x}_0)\|_2, \quad (8)$$

where  $\hat{\beta}(\mathbf{x}_0)$  are the coefficients of the locally weighted linear regression fit to the pairs  $(\mathbf{x}_0^{(j)}, f(\mathbf{x}_0^{(j)}))$ .

Alternatively, a finite-difference approximation may be used, where for each pair of perturbed points  $(\mathbf{x}_0^{(j)}, \mathbf{x}_0^{(k)})$ ,

$$d_{jk} = \frac{|f(\mathbf{x}_0^{(j)}) - f(\mathbf{x}_0^{(k)})|}{\|\mathbf{x}_0^{(j)} - \mathbf{x}_0^{(k)}\|}. \quad (9)$$

The maximal, mean, or quantile value of  $d_{jk}$  over all sampled pairs provides a nonparametric Lipschitz estimate.

Empirically, high Lipschitz values indicate regions where the model's output exhibits steep gradients or rapid transitions, which often correspond to high local uncertainty and unstable explanations. Conversely, small Lipschitz metrics are observed where the model behaves predictably and is less sensitive to local changes. This makes the Lipschitz metric an effective and interpretable diagnostic for pointwise risk and the evaluation of model explainability in nonlinear and high-dimensional settings.

## 5.2 Jaccard Top- $k$ Feature Overlap Metric

The Jaccard metric is employed to assess the compositional stability of feature attributions assigned by local surrogate models. In explainability studies, stability of the set of features deemed “most important” in repeated local explanations is desirable, as it implies interpretative consistency for model users and stakeholders.

For a target instance  $\mathbf{x}_0$ , let  $\mathcal{S}_m$  denote the set of features identified among the top- $k$  by absolute coefficient magnitude in the  $m$ -th local surrogate (such as LIME) fitted at a perturbed instance within the local neighborhood of  $\mathbf{x}_0$ . Typically,  $M$  such perturbations and replicas are considered, yielding sets  $\{\mathcal{S}_1, \mathcal{S}_2, \dots, \mathcal{S}_M\}$ .

The pairwise Jaccard index between two feature sets  $\mathcal{S}_a$  and  $\mathcal{S}_b$  is defined as

$$J(\mathcal{S}_a, \mathcal{S}_b) = \frac{|\mathcal{S}_a \cap \mathcal{S}_b|}{|\mathcal{S}_a \cup \mathcal{S}_b|}. \quad (10)$$

The average pairwise Jaccard index over all pairs of replicates quantifies the overall stability:

$$J_{\text{avg}}(\mathbf{x}_0) = \frac{2}{M(M-1)} \sum_{1 \leq a < b \leq M} J(\mathcal{S}_a, \mathcal{S}_b). \quad (11)$$

In practical code implementations, a matrix of selected top- $k$  features for each local fit is constructed, and the pairwise intersection and union are computed for all replicate pairs. The resulting average index provides a value between 0 (completely different sets for every explanation) and 1 (identical top features for all perturbations).

The Jaccard metric does not measure the magnitude of feature importance, but rather the consistency of feature selection across perturbations. High values of the Jaccard metric indicate that the same features dominate local surrogate explanations, reflecting robust interpretability with respect to the composition of explanations. In contrast, low values suggest compositional instability, indicating that small changes in the input or the local data distribution can yield substantially different attributions, thereby reducing explanation trustworthiness. Notably, the Jaccard metric may become unstable in regions where the model is locally flat, noisy, or when multiple features contribute weakly and interchangeably to the prediction.

### 5.3 Hessian Instability

In practical applications of local surrogate modeling for interpretability, true model instability can arise from both the variability in the strength of explanatory attributions and their shifting patterns of feature interaction. We propose a two-component decomposition of explanatory instability, magnitude and coupling, yielding a robust, unitless stability score when inputs are standardized.

Assume feature inputs are standardized (*mean 0, deviation 1*). Let  $f(x) \approx \alpha_i + \beta_i^\top x$  be the local linear approximation fitted in neighborhood  $i = 1, \dots, m$ , with slope vectors stacked as rows of  $B \in \mathbb{R}^{m \times n}$ . Define the mean slope vector  $\bar{\beta} = \frac{1}{m} \sum_{i=1}^m \beta_i$ , and the centered matrix  $B_c = B - \mathbf{1}\bar{\beta}^\top$ , where  $\mathbf{1}$  is a column vector of ones.

Construct the *slope covariance* matrix:

$$\Sigma_\beta = \frac{1}{m-1} B_c^\top B_c.$$

#### 5.3.1 Hessian Magnitude Instability (Scale Variability)

*Magnitude instability* captures the typical scale of coefficient fluctuation relative to average slope size:

$$I_{\text{mag}} = \frac{\text{tr}(\Sigma_\beta)}{\frac{1}{m} \sum_{i=1}^m \|\beta_i\|_2^2} \in [0, \infty),$$

where  $\text{tr}(\cdot)$  denotes the matrix trace, and both numerator and denominator share units of  $(\text{output})^2$ . This ratio is therefore unitless. The corresponding *magnitude stability* mapping is:

$$S_{\text{mag}} = \frac{1}{1 + I_{\text{mag}}} \in (0, 1].$$

By normalizing by the mean squared slope,  $I_{\text{mag}}$  robustly reflects instability even as the scale of the underlying model varies.

### 5.3.2 Hessian Coupling Instability (Interaction Volatility)

*Coupling instability* quantifies off-diagonal (cross-feature) fluctuations in the coefficient covariance:

$$I_{\text{cpl}} = \frac{\|\Sigma_{\beta} - \text{diag}(\Sigma_{\beta})\|_F}{\|\Sigma_{\beta}\|_F} \in [0, 1], \quad S_{\text{cpl}} = 1 - I_{\text{cpl}},$$

where  $\|\cdot\|_F$  is the Frobenius norm.  $I_{\text{cpl}}$  is unitless by construction, and unlike correlation-based metrics, remains defined even when some input features have negligible variance. High coupling instability reflects the tendency of explanatory features to change together in an unstable or unpredictable way.

### 5.3.3 Hessian Combined Instability Score

Define a unified, unitless *overall stability score*:

$$I_{\text{overall}} = I_{\text{mag}} \times I_{\text{cpl}} \in [0, 1]$$

with  $I_{\text{overall}} = 0$  if and only if  $\Sigma_{\beta} = 0$  (i.e., all local slopes are identical, perfect stability). This multiplicative approach ensures that any substantial volatility in either magnitude or coupling lowers the overall stability score.

This formulation is similar in spirit to explanation consistency and stability analyses proposed in work on explanation robustness [3], which argue that explanations should vary smoothly with the input unless the model itself is inherently discontinuous.

## 6 Empirical Support and Real-World Applications

To evaluate the behavior of uncertainty and explanatory instability in different modeling scenarios, we apply the methodology described above to several illustrative examples chosen to have regions of high curvature or discontinuities. Note that a machine learning model is nothing more than a nonlinear mapping of inputs to output, either via nonlinear functions or segmented linear approximation. Thus, the concepts of uncertainty and explainability can be explored without requiring interesting public data sets on which to train. The commonly referenced public data sets, such as US mortgage defaults, have too little nonlinearity to provide an interesting test case.

## 6.1 Nonlinear Functions for Testing

To assess the dynamics of explanatory instability and forecast uncertainty, we introduce three synthetic nonlinear functions. These functions are defined over a multivariate input vector  $\mathbf{x} \in \mathbb{R}^N$  and chosen to exhibit different forms of local complexity and gradient behavior. For all of the test functions, all input features are randomly sampled from unit normal distributions.

**Wave-like Function** A wave-like function combines smooth saturation with localized oscillations. It is defined as

$$y = w_1 \tanh(5x_1) + w_2 e^{-x_2^2} \sin(10x_2) + w_3 \sin(3x_3) \cos(2x_3) + w_4 x_4 e^{-0.5x_4^2} \quad (12)$$

This function exhibits a steep transition in the  $x_1$  direction due to the hyperbolic tangent, and a band-limited wave in the  $x_3$  direction that is attenuated away from  $x_2 = 0$ .

**Radial Function** The radial function generates spherical symmetry and nonlinear curvature centered at the origin. It is defined as

$$y = \frac{\sin(5\|\mathbf{x}\|)}{1 + 0.5\|\mathbf{x}\|^2}, \quad \text{where } \|\mathbf{x}\| = \sqrt{x_1^2 + x_2^2 + \dots + x_N^2} \quad (13)$$

It features oscillations with decreasing amplitude as the radius increases, creating smoothly varying gradients in all directions.

**Sigmoid Network** The sigmoid network has the form of a typical neural network that is smooth everywhere. Each input dimension is passed through a scaled sigmoid transformation before linear aggregation.

$$y = \sum_{j=1}^N w_j [a_j \cdot \sigma(b_j x_j) + c_j], \quad \text{with } \sigma(x) = \frac{1}{1 + e^{-x}} \quad (14)$$

This formulation introduces variable sharpness and curvature across different dimensions, where the parameters  $a_j$ ,  $b_j$ ,  $c_j$ , and  $w_j$  are randomly sampled for each simulation.

Each of these functions is continuous and differentiable, but exhibits varying levels of local nonlinearity. They are used to test the robustness of local surrogate explanations and highlight conditions under which instability or high uncertainty may arise.

Note that all of these functions are extremely nonlinear compared to a typical credit risk model. This was done to push the limits of uncertainty and explainability.

## 6.2 Piecewise Linear Models

With any segmented modeling approach, the assumption of a locally constant or locally linear structure necessarily becomes inaccurate at the boundaries between segments. Consequently, the explanations from such models are less reliable at the boundaries. Therefore, the same point-wise local-linear analysis as in LIME is a fair test of the reliability of the

forecast uncertainty. Discontinuities at segment boundaries, where intercepts and gradients shift abruptly, fundamentally undermine local linear approximations. These transitions create regions where the assumption of local linearity fails, rendering explanations based upon the segmented linear model unreliable. These concerns apply equally to approaches such as stochastic gradient boosted regression trees [16], ReLU neural networks, and simple segmented logistic regression.

To test the diagnostic utility of these metrics in a controlled setting, we construct a synthetic statistical model where each input  $x_j \sim \mathcal{N}(0, 1)$  for  $j = 1, \dots, 3$ . Each input is passed through a piecewise linear transformation.

$$z_j = \begin{cases} a_j x_j, & \text{if } x_j < 0 \\ b_j x_j, & \text{if } x_j \geq 0 \end{cases} \quad (15)$$

for randomly sampled slopes  $a_j$  and  $b_j$ . The response variable is then computed as a linear combination.

$$y = \sum_{j=1}^3 w_j z_j. \quad (16)$$

Because this system has structural discontinuities at  $x_j = 0$ , we expect elevated instability near those decision boundaries. The empirical results confirm that both uncertainty and  $\log(\text{trace}(\text{Cov}))$  peak near those points, while regions far from the boundaries exhibit stable and low-variance explanations.

### 6.3 Results

Numerical simulations of the four test functions provide clarity on the relationships between metrics that may not be apparent from the algebraic descriptions.

Comparing across test functions, consistent relationships are obtained. Figure 1 shows the relationship between the Hessian magnitude instability measure versus the local linear forecast uncertainty. The best fit line is  $y = \alpha + \beta \log(x)$  with an  $R^2 = 0.983$ . The Hessian magnitude instability is therefore highest (greatest instability) for the greatest forecast uncertainty. The units shown are from the function definition and have no intrinsic meaning. None of the Hessian instability measures have any significant correlation to the conformal forecast uncertainty.

Conversely, Figure 2 shows the relationship between the Lipschitz mean explanatory instability and the conformal forecast uncertainty. The best fit line is again  $y = \alpha + \beta \log(x)$  with an  $R^2 = 0.989$ . Higher conformal uncertainty predicts higher Lipschitz instability. However, the Lipschitz measure exhibit high correlations only to the conformal uncertainty measures and are uncorrelated to the local linear uncertainty.

Not surprisingly, Lipschitz instability and Hessian instability are uncorrelated, just as local linear uncertainty and conformal uncertainty are uncorrelated.

The full set of correlations are given in Table 1. All three Lipschitz metrics were highly intercorrelated, with the simple Lipschitz mean having a slightly higher correlation to the conformal uncertainty. The Hessian magnitude and Hessian coupling were much less correlated, as they measure different information about the test. Hessian magnitude consistently

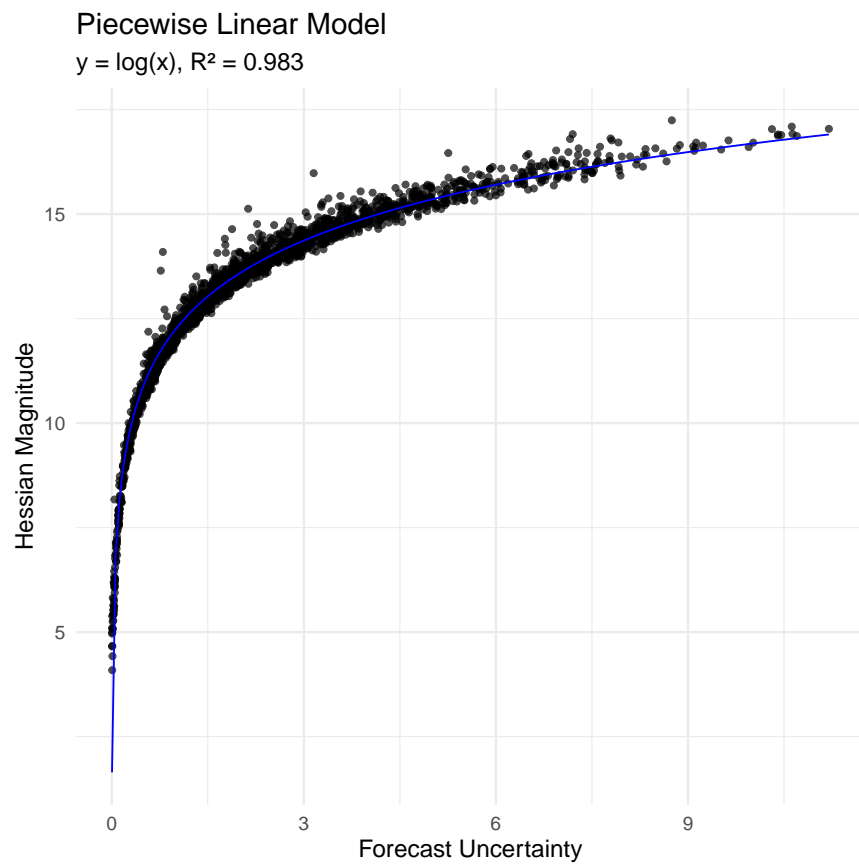


Figure 1: The relationship between Hessian magnitude explanatory instability and local linear uncertainty. Each point is the estimate at one randomly sampled point in the feature space.

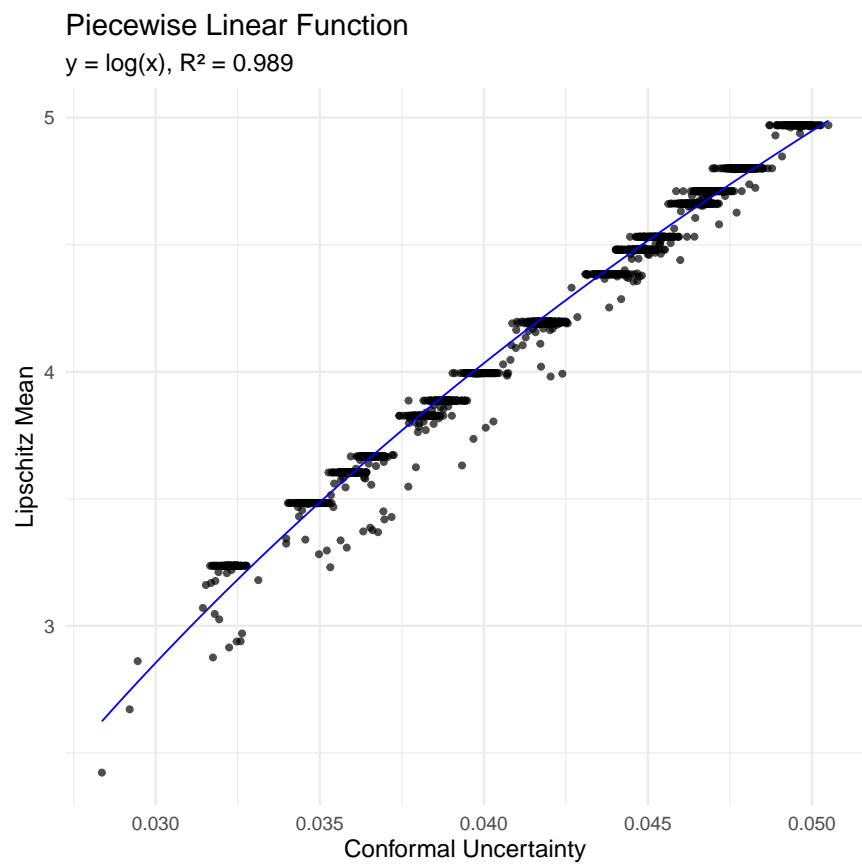


Figure 2: The relationship between Lipschitz explanatory instability and conformal forecast uncertainty. Each point is the estimate at one randomly sampled point in the feature space.

correlates better to local linear uncertainty. The Hessian overall metric does not provide a best-of-both combination, but rather is reduced to match the Hessian coupling correlation.

The Jaccard TopK measure does not correlate to either the Lipschitz or Hessian explanatory instability measures, although it might have been expected to have an anti-correlation to both.

These results provide valuable insights into the relationship between these measures, but they do not determine which is best, because no ground truth for a true value of explanatory instability exists. Rather each of these has theoretical merit and a combination of all could be appropriate.

Perhaps the most intriguing result is that Lipschitz and Hessian measures are highly correlated to distinctly different measures of forecast uncertainty. Conformal forecast uncertainty measures the distribution of forecast values obtained via small perturbations of the input features. Local linear uncertainty measures the degree to which the local neighborhood can be well approximated by a linear model. Thus, conformal uncertainty is the forecast volatility and local linear uncertainty is the linear divergence.

The Lipschitz and Hessian explanatory instability measures both make intuitive sense as measures of explanatory instability, but they exhibit nearly perfect correlations to the respective forecast uncertainty measures. This reinforces the idea that explanatory instability is really a forecast uncertainty issue.

## 7 Theoretical Derivation of the Uncertainty-Instability Relationship

### 7.1 Lipschitz Explanatory Instability and Conformal Uncertainty

The empirical observation of a strong, approximately linear relationship between Lipschitz-based explanatory instability and conformal uncertainty in local model analysis can be supported by a formal mathematical argument, especially in smooth or locally linear regions of a model’s response surface. Consider a predictive function  $f : \mathbb{R}^N \rightarrow \mathbb{R}$  evaluated at a point  $\mathbf{x}_0$ , with explanatory stability and prediction uncertainty assessed via small perturbations of the input.

Suppose that input perturbations are generated as  $\boldsymbol{\epsilon} \sim N(0, \sigma_{\text{pert}}^2 I)$ , so that analysis is confined to a local, isotropic neighborhood around  $\mathbf{x}_0$ . Expanding the model output in a first-order Taylor approximation yields

$$f(\mathbf{x}_0 + \boldsymbol{\epsilon}) \approx f(\mathbf{x}_0) + \nabla f(\mathbf{x}_0)^\top \boldsymbol{\epsilon}. \quad (17)$$

Under this approximation, the variance of the predicted values over the perturbation distribution is given by

$$\text{Var}[f(\mathbf{x}_0 + \boldsymbol{\epsilon})] \approx \text{Var}[\nabla f(\mathbf{x}_0)^\top \boldsymbol{\epsilon}]. \quad (18)$$

Because  $\boldsymbol{\epsilon}$  is Gaussian with zero mean and covariance  $\sigma_{\text{pert}}^2 I$ , it follows that

$$\text{Var}[\nabla f(\mathbf{x}_0)^\top \boldsymbol{\epsilon}] = \nabla f(\mathbf{x}_0)^\top \text{Cov}(\boldsymbol{\epsilon}) \nabla f(\mathbf{x}_0) = \sigma_{\text{pert}}^2 \|\nabla f(\mathbf{x}_0)\|^2, \quad (19)$$

	Function	Lipschitz	Jaccard	Hessian	Hessian	Hessian	Conformal	Local Linear
			TopK	Magnitude	Coupling	Overall	Forecast	Uncertainty,
							Uncertainty	log
Lipschitz	Wave-like	1.0	0.0947	0.0259	-0.0205	-0.0205	0.9998	-0.0006
Jaccard	TopK	0.0947	1.0	-0.0193	-0.0507	-0.0507	0.0904	-0.0249
Hessian	Magnitude	0.0259	-0.0193	1.0	0.5281	0.5281	0.0280	0.9855
Hessian	Coupling	-0.0205	-0.0507	0.5281	1.0	1.0	-0.0188	0.4704
Hessian	Overall	-0.0205	-0.0507	0.5281	1.0	1.0	-0.0188	0.4704
Conformal	Forecast Uncertainty	0.9998	0.0904	0.0280	-0.0188	-0.0188	1.0	0.0014
Local	Linear Uncertainty, log	-0.0006	-0.0249	0.9855	0.4704	0.4704	0.0014	1.0
Lipschitz	Radial	1.0	0.3009	-0.1940	0.0218	0.0218	0.9999	-0.2081
Jaccard	TopK	0.3009	1.0	-0.1970	-0.0049	-0.0049	0.2957	-0.1861
Hessian	Magnitude	-0.1940	-0.1970	1.0	0.1647	0.1648	-0.1917	0.9784
Hessian	Coupling	0.0218	-0.0049	0.1647	1.0	1.0	0.0222	0.0751
Hessian	Overall	0.0218	-0.0049	0.1648	1.0	1.0	0.0222	0.0751
Conformal	Forecast Uncertainty	0.9999	0.2957	-0.1917	0.0222	0.0222	1.0	-0.2060
Local	Linear Uncertainty, log	-0.2081	-0.1861	0.9784	0.0751	0.0751	-0.2060	1.0
Lipschitz	Sigmoid	1.0	0.0705	0.0960	-0.0010	-0.0010	0.9993	0.0952
Jaccard	TopK	0.0705	1.0	0.0646	0.0059	0.0059	0.0701	0.0669
Hessian	Magnitude	0.0960	0.0646	1.0	0.4973	0.4973	0.0968	0.9521
Hessian	Coupling	-0.0010	0.0059	0.4973	1.0	1.0	-0.0011	0.3288
Hessian	Overall	-0.0010	0.0059	0.4973	1.0	1.0	-0.0011	0.3288
Conformal	Forecast Uncertainty	0.9993	0.0701	0.0968	-0.0011	-0.0011	1.0	0.0957
Local	Linear Uncertainty, log	0.0952	0.0669	0.9521	0.3288	0.3288	0.0957	1.0
Lipschitz	Piecewise	1.0	0.1264	0.1518	0.1469	0.1469	0.9958	0.1482
Jaccard	TopK	0.1264	1.0	-0.0110	0.0064	0.0064	0.0858	-0.0095
Hessian	Magnitude	0.1518	-0.0110	1.0	0.4801	0.4801	0.1513	0.9916
Hessian	Coupling	0.1469	0.0064	0.4801	1.0	1.0	0.1459	0.4426
Hessian	Overall	0.1469	0.0064	0.4801	1.0	1.0	0.1459	0.4426
Conformal	Forecast Uncertainty	0.9958	0.0858	0.1513	0.1459	0.1459	1.0	0.1475
Local	Linear Uncertainty, log	0.1482	-0.0095	0.9916	0.4426	0.4426	0.1475	1.0

Table 1: Correlations between explanatory stability metrics, between forecast uncertainty metrics, and between stability and uncertainty metrics.

where  $\|\cdot\|$  denotes the Euclidean norm. Therefore, the standard deviation of model predictions under perturbation, which serves as the conformal estimate of local uncertainty, takes the form

$$\text{SD}_{\text{conf}}(\mathbf{x}_0) \approx \sigma_{\text{pert}} \|\nabla f(\mathbf{x}_0)\|. \quad (20)$$

That is, the conformal uncertainty is proportional to the local Lipschitz constant, with the proportionality constant determined by the scale of perturbation.

In local surrogate analysis, explanatory instability is often proxied by the norm of the coefficients from a locally weighted linear model (such as LIME), which in the small neighborhood limit approaches the gradient, i.e.,  $\|\hat{\beta}(\mathbf{x}_0)\| \approx \|\nabla f(\mathbf{x}_0)\|$ . It follows directly that both explanatory instability and conformal uncertainty reflect the same underlying local sensitivity: the greater the gradient magnitude at a point, the more sensitive the model prediction is to input changes, and the more variable the explanations and outputs become under local perturbations.

While this relationship is exact in the context of linear models and holds very closely for sufficiently small perturbations in smooth nonlinear models, higher-order effects such as curvature (quantified by the Hessian) can introduce mild deviations from strict linearity as the neighborhood radius increases. Nevertheless, for most practical settings involving model diagnosis and local explainability analysis, the theoretical foundation outlined here explains the strong empirical correlation and proportional scaling observed between Lipschitz explanatory instability and conformal uncertainty.

## 7.2 Hessian-Based Instability and Local Linear Uncertainty

The empirical relationships  $\text{Instability} = \alpha + \beta \log \text{Uncertainty}$  observed in Section 6 can be approximately derived from fundamental principles of linear regression uncertainty propagation in a local linear approximation.

In the LIME local approximation, we solve the weighted least squares problem.

$$\hat{\beta} = \arg \min_{\beta} \sum_{i=1}^k w_i [f(\mathbf{z}^{(i)}) - \beta^\top \mathbf{z}^{(i)}]^2 \quad (21)$$

The solution is given by

$$\hat{\beta} = (\mathbf{Z}^\top \mathbf{W} \mathbf{Z})^{-1} \mathbf{Z}^\top \mathbf{W} \mathbf{f} \quad (22)$$

where  $\mathbf{Z}$  is the matrix of perturbed samples  $\mathbf{z}^{(i)}$ ,  $\mathbf{W}$  is the diagonal weight matrix, and  $\mathbf{f}$  is the vector of model evaluations  $f(\mathbf{z}^{(i)})$  [21].

Under the assumption that the local approximation errors  $\varepsilon^{(i)} = f(\mathbf{z}^{(i)}) - \beta^\top \mathbf{z}^{(i)}$  are independent with variance  $\sigma^2$ , the covariance matrix of the coefficient estimates is

$$\text{Cov}(\hat{\beta}) = \sigma^2 (\mathbf{Z}^\top \mathbf{W} \mathbf{Z})^{-1} \quad (23)$$

The key insight is that  $\sigma^2$  represents the variance of the local approximation error, which is directly related to the forecast uncertainty measure [32].

$$\text{Uncertainty}^2 = \frac{\sum_{i=1}^k w_i [f(\mathbf{z}^{(i)}) - \hat{\beta}^\top \mathbf{z}^{(i)}]^2}{\sum_{i=1}^k w_i} \approx \sigma^2 \quad (24)$$

This shows that the Hessian instability measure and local linear forecast uncertainty are both primarily connected to the local variance.

## 8 Fallback and Safe Decision-Making at High-Uncertainty Regions

The preceding analysis demonstrates both practically and theoretically that forecast uncertainty and explanatory instability are related. Rather than focusing on explanatory stability, deployment systems must include forecast uncertainty in the decision logic. When the forecast uncertainty is too high, the primary concern should be in obtaining a usable decision.

Nonlinear machine learning models cannot be expected to provide usable forecasts throughout the feature space, and generally will not when they diverge from simple linear models. When the uncertainty crosses a predefined acceptance threshold, a fallback model should be employed. This necessarily means that all machine learning models should be tested pointwise across the feature space to determine if there are such unpredictable regions. Note that the only machine learning models without such unpredictable regions are essentially linear models and do not need to be deployed as machine learning models.

Upon determining that a machine learning model has prediction gaps, a fallback model will be required. This will most often be a simpler linear model, such as logistic regression with continuous or categorical input features. Such models are unlikely to have predictability gaps. However, they will tend to be less predictive than a machine learning model overall, assuming that overfitting issues have been addressed in the development of the machine learning model [7]. Note that logistic regression models that use features that are segmented continuous variables should be viewed as nonlinear models, not linear models, because they will exhibit the forecast uncertainties at the boundaries exhibited above.

The fallback procedure is dependent on establishing a predetermined maximum threshold for forecast uncertainty. This threshold should be set according to the acceptable level of business risk, and may be a function of the forecast value. For example, a large uncertainty in a low credit default risk situation could be irrelevant, whereas a large uncertainty in a high default risk could be disastrous. However, with a risk-based pricing approach, losing profitability could happen at either end of the spectrum or in specific segments.

## 9 Conclusions

As noted, previous studies have connected uncertainty and explainability, although operational aspects of this have been missed. Rather than the industry focus on explainability, loan origination must explicitly take forecast uncertainty into account. Explanatory instability is a minor concern once the unforecastable points have been resolved. The present work also provides novel metrics for explanatory instability that capture aspects of the problem not identified by previous metrics.

The simulation and theoretical results also provide insight into what to expect from machine learning models and how to work with their limitations in practice. Importantly, this work proves the intuition that machine learning models do not have the slowly varying

forecast uncertainty that business owners have come to expect from experiences using logistic regression scores. The variability of forecast uncertainty is underappreciated and almost never incorporated into the underwriting process, creating a significant risk of model misuse. The ability to find pockets of predictability in high-dimensional, complex feature spaces is a great asset. Ignoring the unpredictable pockets creates significant risk.

Just as important is to set aside the notion that piecewise linear models are somehow more explainable than continuous nonlinear models. This is only true toward the centers of those segments. Near the boundaries, variation in the inputs causes boundary crossings that demonstrate the uncertainty and instability of the models. In fact, a well-trained piecewise linear model will place those boundaries exactly at the high curvature regions of a nonlinear, continuous model. Thus both models, when well-trained, will exhibit uncertainty and instability in the same feature space regions. The explanatory power of piecewise linear models is illusory.

Although this work was first motivated by the question of how to make machine learning models explainable, as often happens in science, the solution was to change the question. Not only must we accept that many forecasts do not have explanatory stability, but those same forecasts are seldom usable because of the inherent uncertainty. This was demonstrated via simulation and theoretical derivation.

In all of the examples simulated here, the input features are independent, as are the perturbations applied. In a realistic model, both of those may be untrue, which may introduce additional structure or noise in the uncertainty - instability relationships. Such dependence between features may also violates the theoretical considerations.

In such inherently unpredictable situations, the lender might wish to reject the applicant on the basis of insufficient information. However, regulators may find forecast uncertainty to be an unacceptable justification for rejection to consumers. The lender then has a choice of biasing their underwriting decisions to accept applicants with uncertain forecasts or to maintain a simpler forecasting model that follows traditional behavior patterns. The choice should be driven by financial consequences, not a failure to understand the models.

## References

- [1] Julius Adebayo, Justin Gilmer, Michael Muelly, Ian Goodfellow, Moritz Hardt, and Been Kim. Sanity checks for saliency maps. In *Advances in Neural Information Processing Systems (NeurIPS)*, 2018.
- [2] David Alvarez-Melis and Tommi S Jaakkola. On the robustness of interpretability methods. *arXiv preprint arXiv:1806.08049*, 2018.
- [3] David Alvarez-Melis and Tommi S Jaakkola. Towards robust interpretability with self-explaining neural networks. In *Advances in Neural Information Processing Systems*, 2018.
- [4] Raman Arora, Amitabh Basu, Poorya Mianjy, and Anirbit Mukherjee. Understanding deep neural networks with rectified linear units. *arXiv preprint arXiv:1611.01491*, 2016.

- [5] Christopher M. Bishop. Bayesian neural networks. *Journal of the Brazilian Computer Society*, 4(1):31–38, 1997.
- [6] Joseph L. Breeden. A survey of machine learning in credit risk. *Journal of Credit Risk*, 17(3), 2021.
- [7] Joseph L Breeden and Yevgeniya Leonova. Stabilizing machine learning models with age-period-cohort inputs for scoring and stress testing. *Frontiers in Applied Mathematics and Statistics*, 9:1195810, 2023.
- [8] Leo Breiman. Statistical modeling: The two cultures. *Statistical Science*, 16(3):199–231, 2001.
- [9] Rich Caruana, Yin Lou, Johannes Gehrke, Paul Koch, Marc Sturm, and Noemie Elhadad. Intelligible models for healthcare: Predicting pneumonia risk and hospital 30-day readmission. In *Proceedings of the 21th ACM SIGKDD international conference on knowledge discovery and data mining*, pages 1721–1730, 2015.
- [10] Yue Chen et al. Estimating neural network robustness via lipschitz constant and curvature. *arXiv preprint arXiv:2311.01424*, 2023.
- [11] Osman Denas et al. Feature importance in interpretable models: An empirical comparison of methods. In *ICLR Workshop on "SafeAI"*, 2021.
- [12] Hongyin Dong et al. Rashomon sets: Closing the gap between robustness and interpretability. In *AAAI*, 2020.
- [13] Toby J. Fel et al. Effective pruning for top-k feature search on the basis of feature stability. *Progress in Artificial Intelligence*, 2024.
- [14] Aaron Fisher et al. All models are wrong, but many are useful: Learning a diverse set of accurate and interpretable models. In *ICML*, 2019.
- [15] FRB. Supervisory guidance on model risk management. Technical report, Board of Governors of the Federal Reserve System, April 2011.
- [16] Jerome H Friedman. Stochastic gradient boosting. *Computational statistics & data analysis*, 38(4):367–378, 2002.
- [17] Yarin Gal and Zoubin Ghahramani. Dropout as a bayesian approximation: Representing model uncertainty in deep learning. In *Proceedings of the 33rd International Conference on Machine Learning*, pages 1050–1059. PMLR, 2016.
- [18] Jakob Gawlikowski, Cedrique Rovile Njieutcheu Tassi, Mohsin Ali, Jongseok Lee, Matthias Humt, Jianxiang Feng, Anna Kruspe, Rudolph Triebel, Peter Jung, Ribana Roscher, et al. A survey of uncertainty in deep neural networks. *Artificial Intelligence Review*, 56(Suppl 1):1513–1589, 2023.
- [19] Ethan Goan and Clinton Fookes. Bayesian neural networks: An introduction and survey. *arXiv preprint arXiv:2006.12024*, 2020.

- [20] Chuan Guo, Geoff Pleiss, Yu Sun, and Kilian Q. Weinberger. On calibration of modern neural networks. *International Conference on Machine Learning (ICML)*, 2017.
- [21] Trevor Hastie, Robert Tibshirani, Jerome Friedman, et al. The elements of statistical learning, 2009.
- [22] Sara Hooker et al. A benchmark for interpretability methods in deep neural networks. In *NeurIPS*, 2020.
- [23] Roger Koenker and Gilbert Bassett Jr. Regression quantiles. *Econometrica*, 46(1):33–50, 1978.
- [24] Balaji Lakshminarayanan, Alexander Pritzel, and Charles Blundell. Simple and scalable predictive uncertainty estimation using deep ensembles. In *Advances in Neural Information Processing Systems (NeurIPS 2017)*, pages 6402–6413, 2017.
- [25] Zachary C Lipton. The mythos of model interpretability. *Queue*, 16(3):31–57, 2018.
- [26] Scott M. Lundberg and Su-In Lee. A unified approach to interpreting model predictions. *Advances in Neural Information Processing Systems (NeurIPS)*, 2017.
- [27] Nijat Mehdiyev, Maxim Majlatow, and Peter Fettke. Quantifying and explaining machine learning uncertainty in predictive process monitoring: an operations research perspective. *Annals of Operations Research*, pages 1–40, 2024.
- [28] Radford M. Neal. *Bayesian Learning for Neural Networks*. Springer Science & Business Media, 2012.
- [29] Harsha Nori, Samuel Jenkins, Paul Koch, and Rich Caruana. Interpretml: A unified framework for machine learning interpretability. *arXiv preprint arXiv:1909.09223*, 2019.
- [30] OCC. Supervisory guidance on model risk management. Technical report, Office of the Comptroller of the Currency, April 2011.
- [31] Pascal Pernot. Calibration in machine learning uncertainty quantification: beyond consistency to target adaptivity. *APL Machine Learning*, 1(4), 2023.
- [32] Marco Tulio Ribeiro, Sameer Singh, and Carlos Guestrin. Why should i trust you?” explaining the predictions of any classifier. In *Proceedings of the 22nd ACM SIGKDD international conference on knowledge discovery and data mining*, pages 1135–1144, 2016.
- [33] Marco Tulio Ribeiro, Sameer Singh, and Carlos Guestrin. Why should i trust you? explaining the predictions of any classifier. In *Proceedings of the 22nd ACM SIGKDD International Conference on Knowledge Discovery and Data Mining*, pages 1135–1144, 2016.
- [34] Cynthia Rudin. Stop explaining black box machine learning models for high stakes decisions and use interpretable models instead. *Nature Machine Intelligence*, 1(5):206–215, 2019.

- [35] Massimo Salvi, Silvia Seoni, Andrea Campagner, Arkadiusz Gertych, U.Rajendra Acharya, Filippo Molinari, and Federico Cabitza. Explainability and uncertainty: Two sides of the same coin for enhancing the interpretability of deep learning models in healthcare. *International Journal of Medical Informatics*, 197:105846, 2025.
- [36] Miguel Sanchez et al. Evaluation metrics for explanations in xai: practical challenges and recommendations. *Frontiers in Artificial Intelligence*, 2022.
- [37] Arthur Thuy and Dries F Benoit. Explainability through uncertainty: Trustworthy decision-making with neural networks. *European Journal of Operational Research*, 317(2):330–340, 2024.
- [38] Berk Ustun, Alexander Spangher, and Yang Liu. Actionable recourse in linear classification. In *Proceedings of the Conference on Fairness, Accountability, and Transparency (FAccT)*, pages 10–19, 2019.
- [39] Vladimir Vovk, Alexander Gammerman, and Glenn Shafer. *Algorithmic Learning in a Random World*. Springer, 2005.
- [40] Sandra Wachter, Brent Mittelstadt, and Chris Russell. Counterfactual explanations without opening the black box: Automated decisions and the GDPR. *Harvard Journal of Law & Technology*, 31(2):841–887, 2018.
- [41] Tsui-Wei Weng et al. Evaluating the robustness of neural networks: An extreme value theory approach. In *International Conference on Learning Representations (ICLR)*, 2018.
- [42] Qiyu Yang et al. On infidelity and sensitivity of feature importance explanations. *IEEE Transactions on Knowledge and Data Engineering*, 2022.
- [43] Chengchun Shu Yeh et al. Fidelity and sensitivity of explanations. In *NeurIPS*, 2019.
- [44] Zhiwei Steven Zhao and Trevor Hastie. The rashomon effect and model reliance: Assessing the ability of variable importance measures to identify relevant variables. In *NeurIPS*, 2021.